Available online at www.CivileJournal.org

Civil Engineering Journal

(E-ISSN: 2476-3055; ISSN: 2676-6957)

Vol. 8, No. 03, March, 2022

Slope Reinforcement Model Scale Test With X-Block

Enos Karapa [1*], Tri Harianto [1], A. B. Muhiddin [1], Rita Irmawaty [1]

[1] *Department of Civil Engineering, Hasanuddin University, Makassar 90245, Indonesia.*

Received 18 December 2021; Revised 08 February 2022; Accepted 19 February 2022; Published 01 March 2022

Abstract

This study aims to determine the material composition and dimensions of X-block, develop a slope reinforcement model using X-block, evaluate the mechanical behavior of slopes that are reinforced with rock-bound by X-block, and analyze the performance of slope reinforcement using X-block. This research was conducted at Hasanuddin University's soil mechanics and civil engineering structure laboratory. The model scale test was employed in this study. The geometrical speciation of the test box is 150 cm in length, 60 cm in width, and 100 cm in height. The X-block model was produced using concrete with a FC of 25 MPa. The X-block was divided into two types: X-block type 1 and X-block type 2. Tensile strength testing is performed on the X-block. The slopes are made of clay soil and have a slope angle of 70 degrees. The loading test was conducted in three stages: without block, with X-block type 1, and with X-block type 2. The loading test uses a hydraulic pump equipped with a load cell and LVDT. The tensile strength of X-block type 1 is 2.56 MPa, whereas X-block type 2 has a tensile strength of 4.35 MPa. The development of the type X-block design, which is used as a retaining wall material, has shown that it can effectively withstand landslides on the slopes under consideration. The slope safety factor rose dramatically after being reinforced with type X-blocks, reaching 2.73 for both X-block type 1 and X-block type 2.

Keywords: X-block; Slope Reinforcement; Slope Stability; Landslides.

1. Introduction

Landslides inflict significant damage and occur in a variety of locations across the world [1]. Landslides cause economic damage and deaths that are understated in certain nations. Catastrophes: Landslides cause more damage than other natural disasters, such as earthquakes, floods, and windstorms [2]. Landslides have also occurred in different places in Indonesia, with negative consequences in a variety of domains, including the ecological, social, and economic. Landslides can happen in many different ways because of the same thing that causes them (e.g., rainstorms, long periods of rain) [3].

Problematic soil (soft soil) usually necessitates the use of a soil treatment technology. One of the soil-reinforcing approaches is the use of wood as a raft foundation material [4]. Landslides can occur as a result of erosion on the surface of a slope. Although erosion is a well-known natural phenomenon, it is sometimes worsened by human activities such as poor land use, deforestation, mining, plantations, farming, poorly managed building and development operations, and road construction [5]. Initial subgrade deformation of the slope's surface layer is common, especially after receiving loads from the construction above it. Slope failure can be caused by land subsidence, particularly in areas prone to settlement, such as clay soil [6]. Reduced slope surface erosion is one of the slope management approaches. Plant

* Corresponding author: karapae17d@student.unhas.ac.id

http://dx.doi.org/10.28991/CEJ-2022-08-03-014

medium or vegetative approaches have been used to manage slope surface erosion. The carrying capacity of the subgrade is the key issue for infrastructure construction in soft clay soils, since the subgrade compaction is rather substantial, implying that it will endure longer. This issue can be rectified by strengthening the soil to make it stronger [7, 8].

The stability of a building is affected by soil conditions. Soil stabilization must be done both physically and chemically to raise the mechanical strength of the soil. Another type of mechanical soil enhancement is stone columns [9]. In addition to employing plant medium, slope erosion may be controlled with a versatile kind of slope protection known as riprap structures. Retaining walls, the most prevalent of which are gravity-retaining stone walls, are typically built around the borders of streams [10]. Overcoming damage to roads and slopes in distant places is still frequently done with soil-based pavement. This is because bringing in adequate materials is expensive [11]. Based on the aforementioned, it is important to install X-block concrete supports to strengthen the gravity wall construction and prevent failure.

2. Literature Review

2.1. Slope Stability

With a history dating back more than 300 years, slope stability is one of the most significant subjects in engineering geology. Various stability assessment techniques have been developed thus far, including simple assessments, planar failure, limit state criteria, limit equilibrium analysis, numerical methods, hybrid and high-order approaches. The interaction between driving and resisting forces is fundamental to slope stability. Some elements contribute to the pushing force, whereas others contribute to the repelling force. As a result, these controlling parameters are critical for rock slope stability analyses in general, and for failure plane modes in particular. Internal regulatory elements include slope geometry, probable failure region features, surface drainage, and groundwater conditions [12], whereas external influences include rainfall, seismicity, and man-made activities [13]. The intensity of rainfall exacerbates the problem of slope stability [14]. This is obvious since slope failure rises during the wet season. These criteria, when considered together, will be accountable for defining the state of slope stability.

Identification of such slope instability problems during the early stages of engineering structure planning and investigation, particularly road projects, may lead to the development of remedial measures that can be adopted to improve slope stability, or such problem slopes can be avoided if identified during the early planning stages [15]. Deterministic slope stability analysis methodologies are time-consuming and need a thorough grasp of geological and geotechnical issues, as well as a comprehensive comprehension of the probable causes of slope failure. Furthermore, these analytical tools can only be applied to limited regions on a single slope scale [16].

In some circumstances, the existence of an underground aquifer supplied by an upstream hydraulic recharge area may be a risk issue for such activity, as it is responsible for deep piezometric heads that can fluctuate seasonally [17]. Many researches have examined the mechanism of the influence of temperature and saturation on unsaturated clay slope stability in light of clay slope instability induced by ambient temperature and rainfall infiltration in summer and autumn [18, 19]. The slope's factor of safety may be calculated by gradually diminishing the soil shear strength until the slope fails. The resultant safety factor is the ratio of the actual shear strength of the soil to the decreased shear strength upon failure. This "shear strength reduction methodology" offers several benefits over slope stability analysis using the slices method. Aside from shear strength, cohesion is among the most crucial elements influencing slope stability [20-22].

2.2. Flexible Slope Reinforcement

Simple slope reinforcement methods, such as gabions, gravity barriers, and riprap, have been widely employed. Gabions are soil reinforcement structures made of woven steel wire coated with zinc and filled with chipped stones in certain proportions. Gabions have several advantages, including simplicity of construction, structural stability, flexibility, and resistance to water loads [23]. Rock riprap is often employed to protect embankments, steep channels, and other structures from damaging overflow erosion [24]. While the soil nailing system is a technology for improving the soil that is used to stabilize slopes. The soil nailing system's behavior is determined by soil types and nailing parameters such as nail spacing, orientation, length, and technique of installation of nails, soil qualities, slope height and angle, and surcharge loading, among others [25].

2.3. Concrete Block Structure

Slope stabilization using concrete blocks is still rather uncommon. Concrete is the most frequently used substance on the planet, with yearly worldwide output estimated to be more than 2 billion cubic meters. Concrete is a hardened substance composed of cement, water, fine aggregate, and coarse aggregate [26]. The application is mainly confined to managing river slopes, although it is nearly never encountered on slopes without drainage and with considerable slope angles.

3. Material and Methods

The research method utilized will define the subject of study, the equipment and materials used, the research plan, and the analysis of any difficulties encountered during the research process.

3.1. Sampling Location

The material applied to set up the slopes is a soft soil type acquired from landslide-prone locations. Figure 1 depicts the site of the land acquisition in Sapaya village, Gowa Regency, South Sulawesi, Indonesia. The coordinates of the sampling site are 5° 21' 44.8" S and 119° 42' 58.7" E.

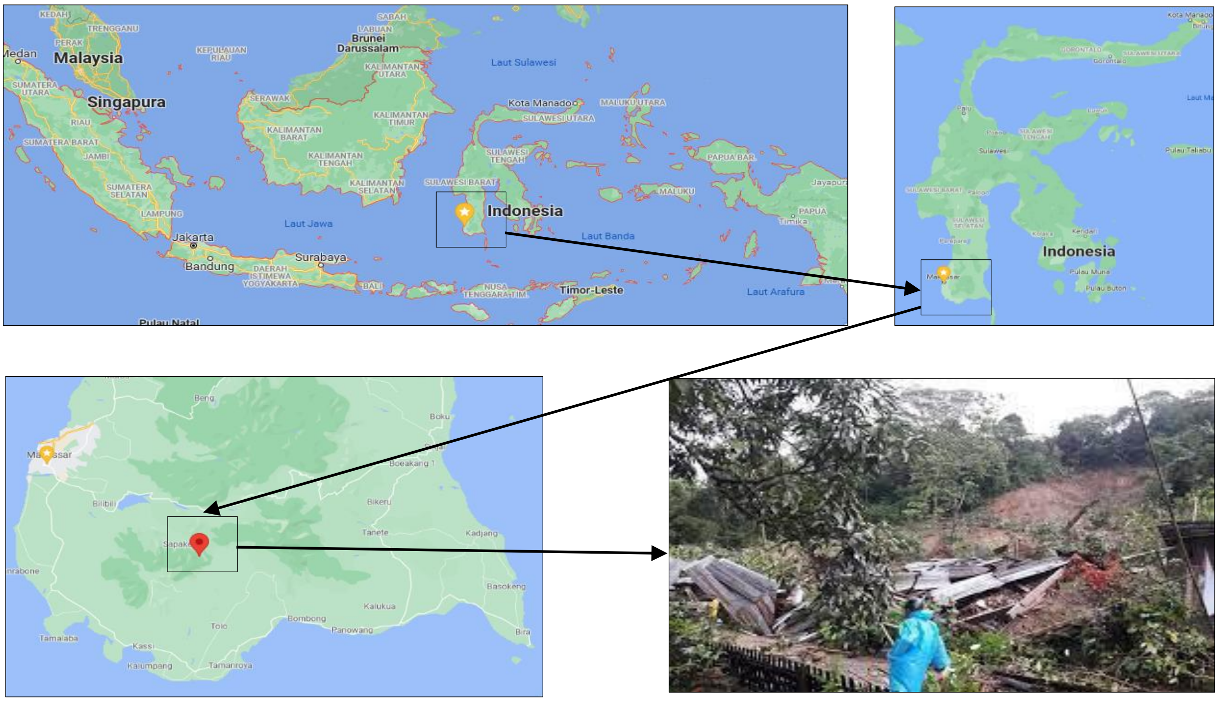

Figure 1. Soil sampling location in Sapaya village, Gowa regency, South Sulawesi, Indonesia

3.2. Materials and Method

An overview with geometric specifications along with other details of the experimental model is shown in Figure 1.

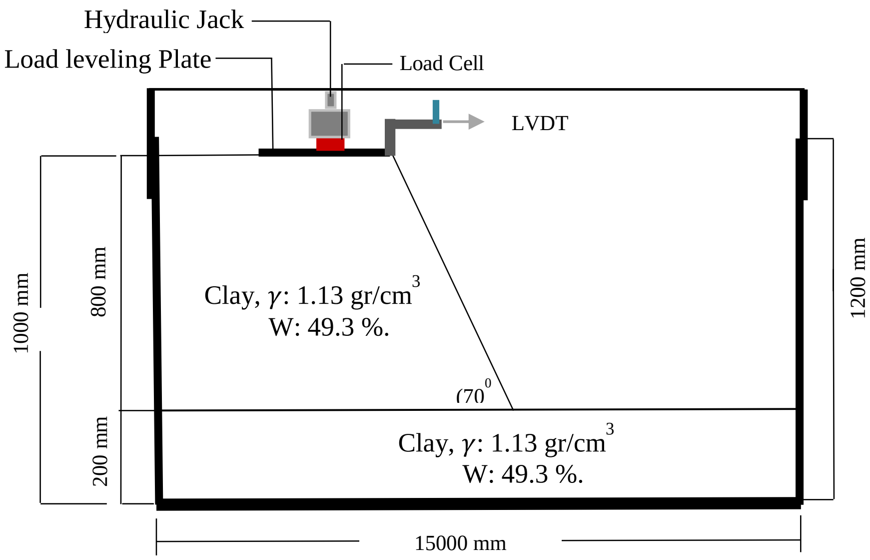

Figure 2. Slope test scheme

The materials employed in this study include laboratory testing standards materials and equipment, which are as follows:

- The type of soil that will be utilized to construct the slope is clay soil. First, it is tested in a soil mechanics laboratory to determine gradation, moisture content, the Atterberg limit (liquid limit, plastic limit, plastic index), maximum dry density, soil density, and optimum moisture content
- 1500 mm (length) × 1200 mm (height) × 600 mm (width) test box;
- Load cell instrument, 200 kN cap;
- 200 mm Sensor Linear Variable Differential Transformers (LVDT);
- Load levelling plate (300×200 mm);
- Hydraulic Pump;
- Compressor.

Figure 3 depicts the testing preparation stage, where the observation equipment, such as load cells, LVDTs, and hydraulic pumps, has been correctly prepared. To read the data, use a computer device that is directly linked to the loading device and LVDT.

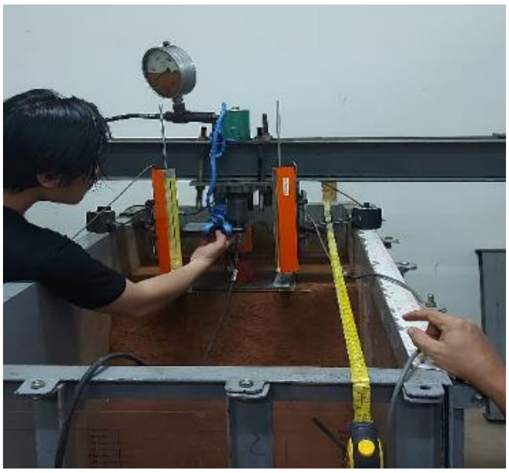

Figure 3. Equipment used in research (Load cell and LVDT circuit)

3.3. Testing Stage

The stages of testing carried out are divided into three stages according to the research design.

Basic Test: The basic test is a clay soil properties test. The purpose of the properties analysis is to investigate the attributes of clay soil which will be utilized in slope test.

Model Test: The model test is the primary testing stage in this study. The installation of X-blocks type 1 and X-blocks type 2 is done alternately, as indicated in Figure 4. A hydraulic pump is used to power the test model, which is a statically loaded slope test model. This test is performed in three stages: 1. without block, 2. with X-Block Type 1, and 3. with X-Block Type 2.

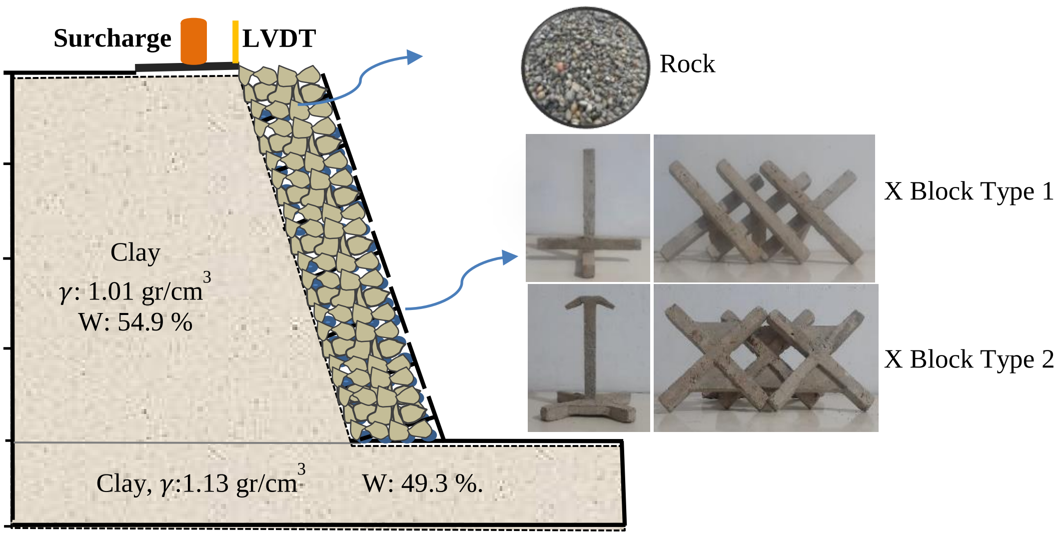

Figure 4. Loading test diagram with X-block reinforcement

4. Results and Discussion

According to the findings of the soil characteristics test, the soil used as a medium for building slopes has a silt composition of 55.28 percent, a cohesiveness value of 0.91 kg/cm^2, and an internal shear angle of 25.06$^{o.}$ Loading tests on untreated slope results in collapses or avalanches. Soil movement begins at the top of the slope and extends to a depth of 500 mm. As indicated in Figure 5, the maximum landslide depth is 200 mm at the top of the slope and the smallest depth is 35 mm at a height of 400 mm from the slope's foot. This avalanche is classified as a block slide based on the type of movement. Based on its pace, this avalanche falls within the category of rapid avalanche.

Table 1. Soil Properties Test Results

Index Properties		Unit	Value
Specific Gravity		-	2.62
Natural State (Soil Index)	Water Content (w)	%	37.31
	Wet Density (γ_{wet})	gr/cm^3	1.54
	Dry Density (γ_{dry})	gr/cm^3	1.12
	Void ratio (e)	-	1.33
	Porosity (n)	-	57.12
	Degree of Saturation (Sr)	%	73.44
Atterberg Limits	Liquid Limit (LL)	%	48.56
	Plastic Limit (PL)	%	40.00
	Plasticity Index (PI)	%	8.56
	Shrinkage Limit (SL)	%	30.10
Grain Size	Gravel	%	0.40
	Sand	%	6.60
	Silt	%	55.28
	Clay	%	37.72
USCS	Soil Classification	-	ML
UCT	UCT (Unconfined Compressive Test)	kg/cm^2	0.260
Direct Test	Cohesion (C)	kg/cm^2	0.91
	Friction Angle (φ)	degree	25.06
Compact Test	Optimum Moisture Cont. (w_0)	%	43.32
	Maximum Dry Density (g_{dry})	t/m^3	1.21

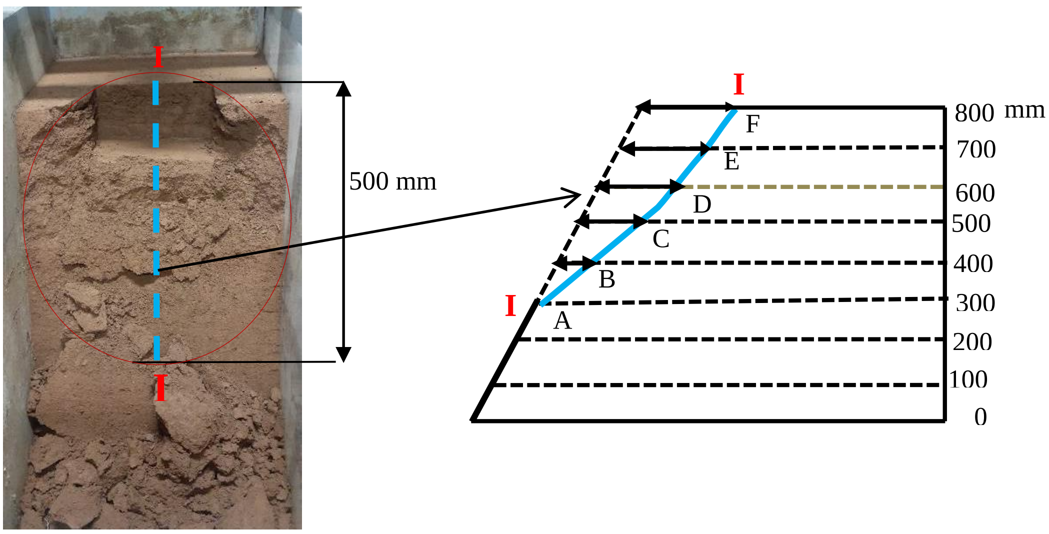

Figure 5. Deformation of the sliding surface (Section I–I)

Figure 6 shows a horizontal and vertical comparison of the deformation of the reinforced slope against the unreinforced slope. The load reached 7.4 kN just before the slope surface collapsed, generating a horizontal deformation of 20 mm. Meanwhile, the X-block types 1 and 2 barely move 1 mm under the same force. The load as an extrinsic element and the nature of the soil as an intrinsic component create the landslide. Slippage occurs as a result of the applied load causing high shear stress. Soil properties with low cohesion and low soil density are intrinsic factors for landslides. The graph above depicts the phenomena of land subsidence followed by landslides, which is a description of landslides induced by the constant rise in load via hydraulic pumps. The maximum load that the slope could withstand before a landslide occurs is 7.4 kN, or equivalently 120 kPa.

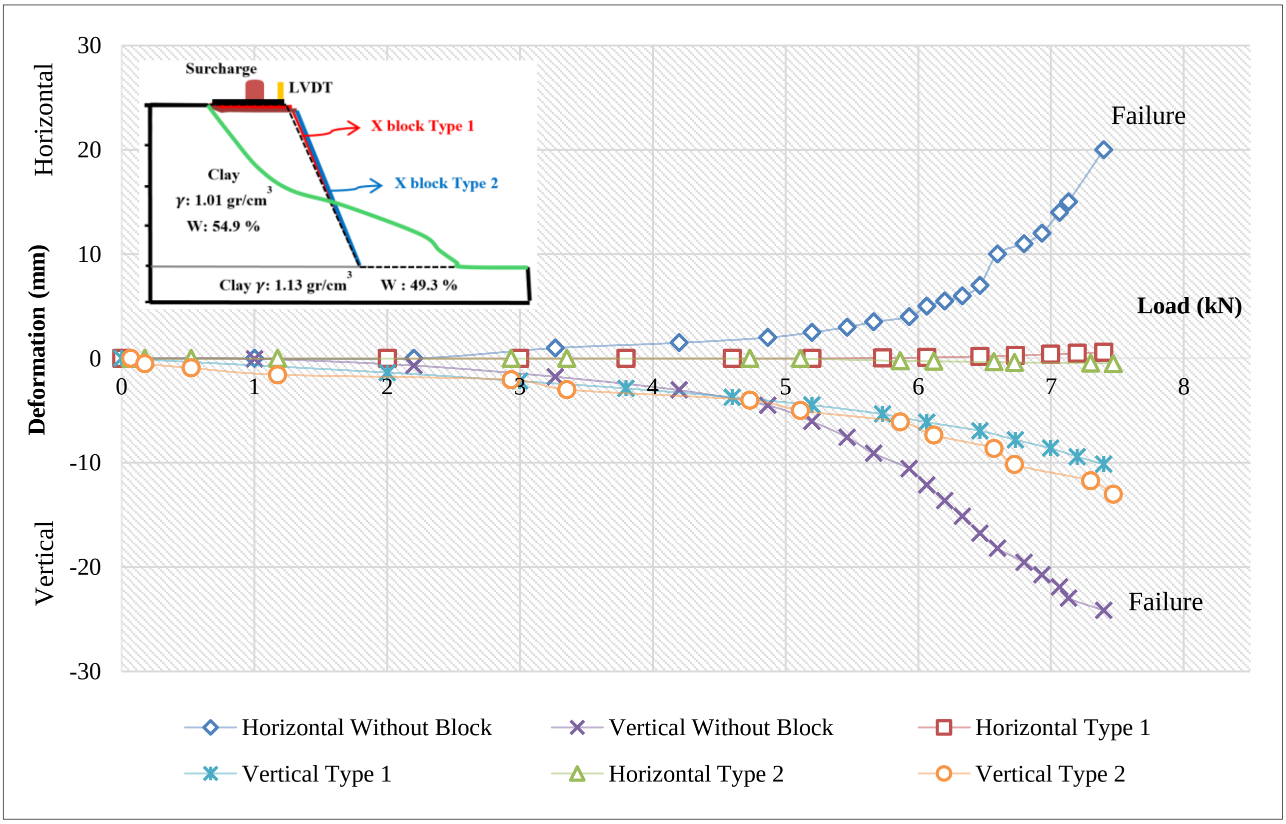

Figure 6. Slope deformation at 7.4 kN surcharge load

Figure 6 also illustrates that reinforcing the slopes using X-block types 1 and 2 is quite effective. With a load of 7.4 kN, the horizontal deformation (h) to slope height (H) ratio is 0.001 for both X-block types. While the vertical deformation (v) to slope height (H) ratio is X-block type 1 of 0.012 and X-block type 2 of 0.016.

Figure 7 depicts a comparison of horizontal and vertical deformations under the ultimate load. The ultimate load without reinforcement is 7.4 kN, the utmost load with reinforcement using X-block type 1 is 18 kN, and the ultimate load with reinforcement using X-block type 2 is 16 kN. The horizontal deformation without reinforcement is 20 mm, the horizontal deformation with reinforcement using X-block type 1 is 40 mm, and the horizontal deformation with reinforcement using X-block type 2 is 50 mm. The unreinforced vertical deformation is 24 mm, 115 mm for X-block type 1, and 123 mm for X-block type 2. The vertical and horizontal deformation graphs presented above can be used to examine slope characteristics reinforced using X-blocks. It demonstrates that the slope condition is still stable while being constantly loaded up to a load of 18 kN for X-block type 1 and a load of 16 kN for X-block type 2. Because the weight of X-blocks and stones as a unit provides a resisting force, slope stability improves with their strengthening. Furthermore, the self-compacting action of stone material with X-blocks is becoming denser, which increases the stiffness attributes of the reinforcement. The safety factor produced by the strengthening of X-block types 1 and 2 is 2.73. (Greater than the standard of 2).

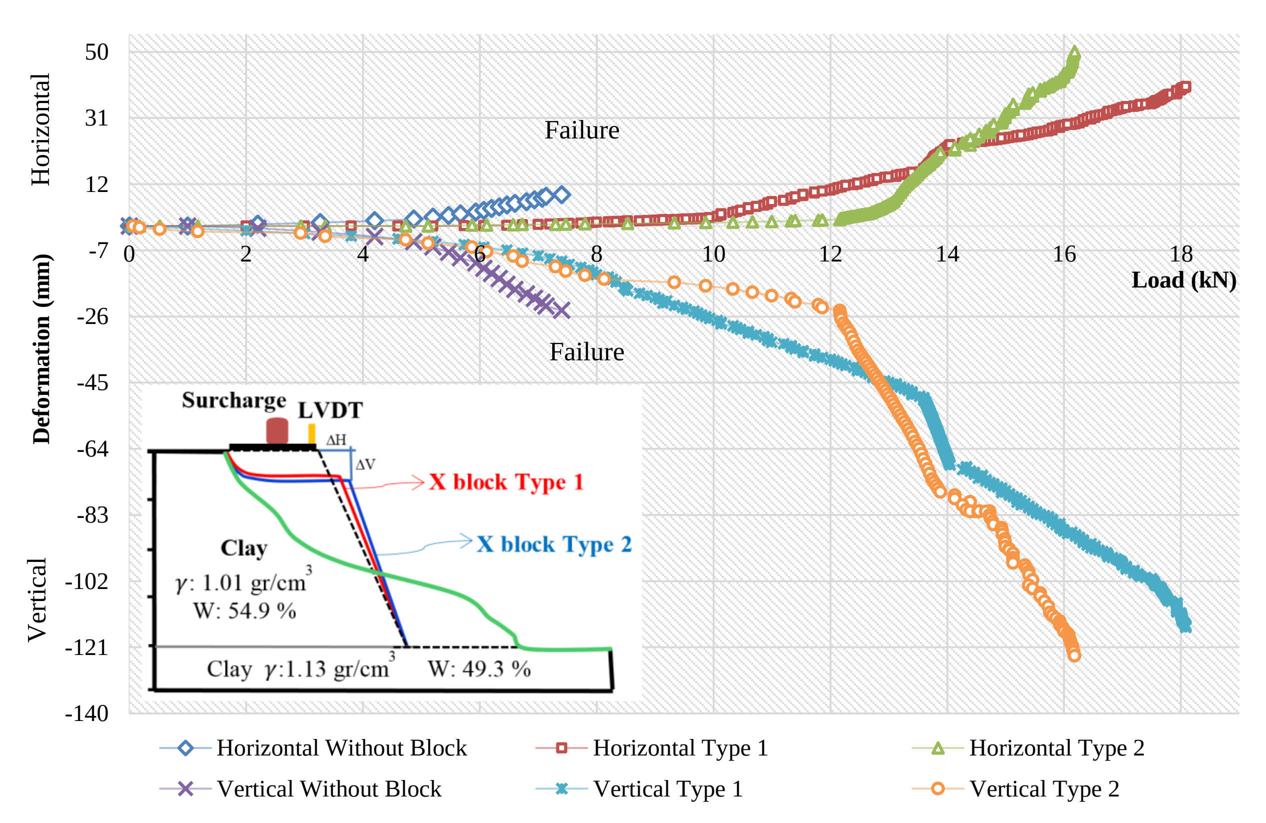

Figure 7. Horizontal and vertical deformation at ultimate load

Figure 8 depicts horizontal distortion in height variations. Deformation varies from a maximum height of 800 mm to a height of 200 mm, with X-block type 2 experiencing higher deformation than X-block type 1 at each height variance. Table 2 shows the amount of deformation at different heights.

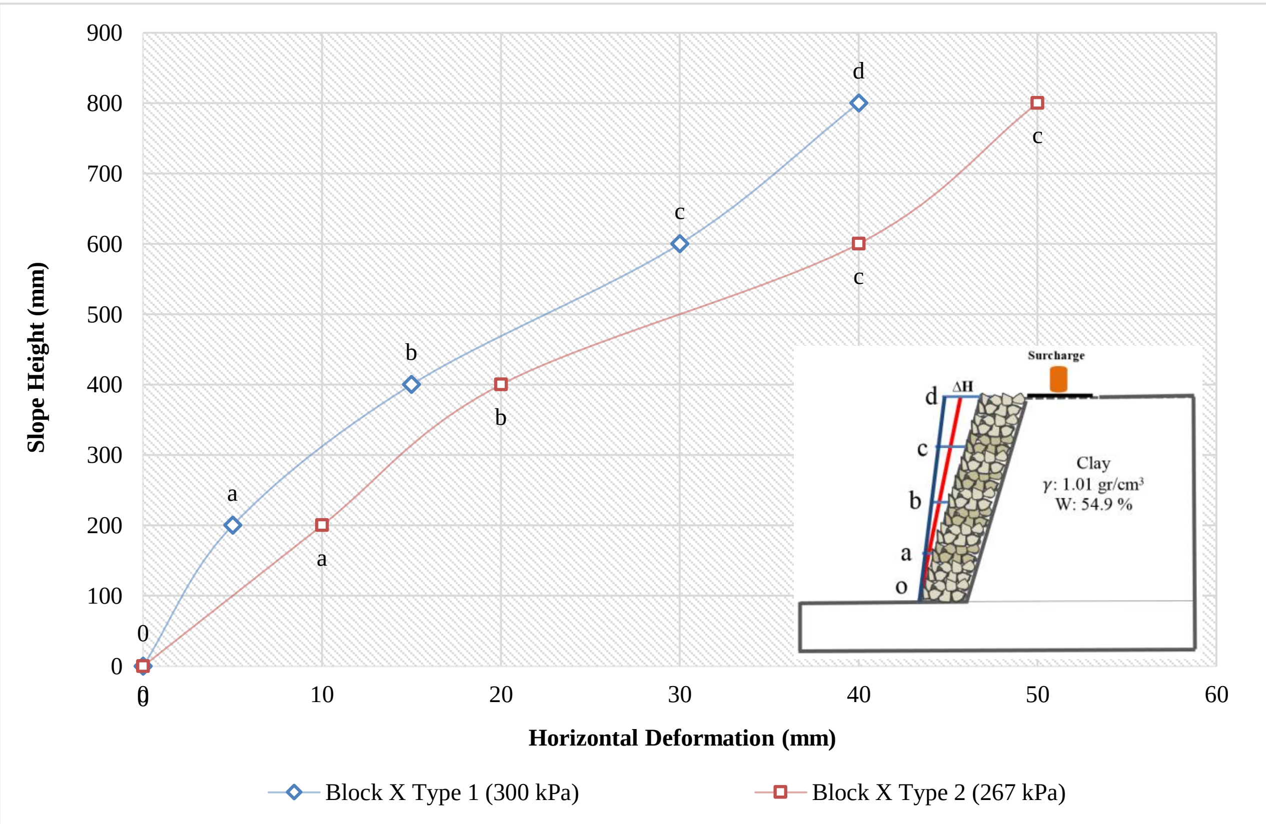

Figure 8. Comparison of the horizontal deformation between type 1 and type 2 X-blocks

Table 2. Horizontal deformation of X type 1 and X type 2 block walls in varied height

Height (mm)	Horizontal deformation (mm)	
	X-block Type 1	X Blok Type 2
800	40	50
600	30	40
400	10	20
200	5	10

Figure 9 depicts the horizontal and vertical deformation to slope height ratios at maximum load for each X-block. The obtained findings reveal that the horizontal deformation ratio of an X type 1 block is 0.050, that of an X type 2 block is 0.063, and that the vertical deformation ratio of an X type block is 0.050. The value for X-block type 1 is 0.144, while the value for X-block type 2 is 0.154. Based on these values, the horizontal deformation value is quite minimal when compared to the height of the slope. This also shows that X-Block type 1 performs better as slope reinforcement than X-Block type 2 since it has a lower horizontal and vertical deformation ratio.

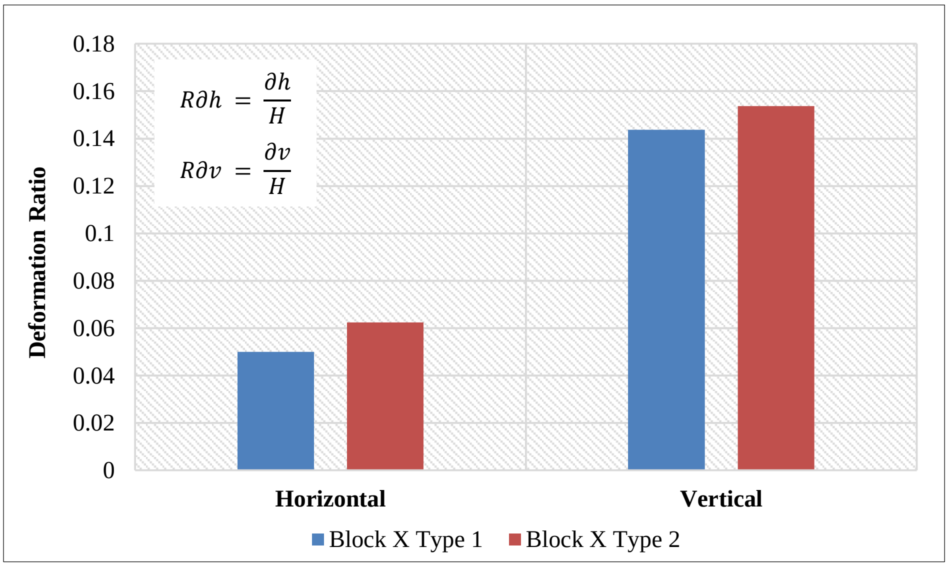

Figure 9. Ratio of horizontal and vertical deformation to slope height

As shown in Figure 10, the rise in slope stability based on the ratio of the X-block reinforcement's ultimate load ratio and the load just before failure is 2.4 for the X-block type 1 reinforcement and 2.2 for the X-block type 2 reinforcement. The value of this ratios indicates that the X-type blocks 1 and 2 could sustain a load twofold the failure load. This number also demonstrates that X-Block type 1 is more effective than X-Block type 2.

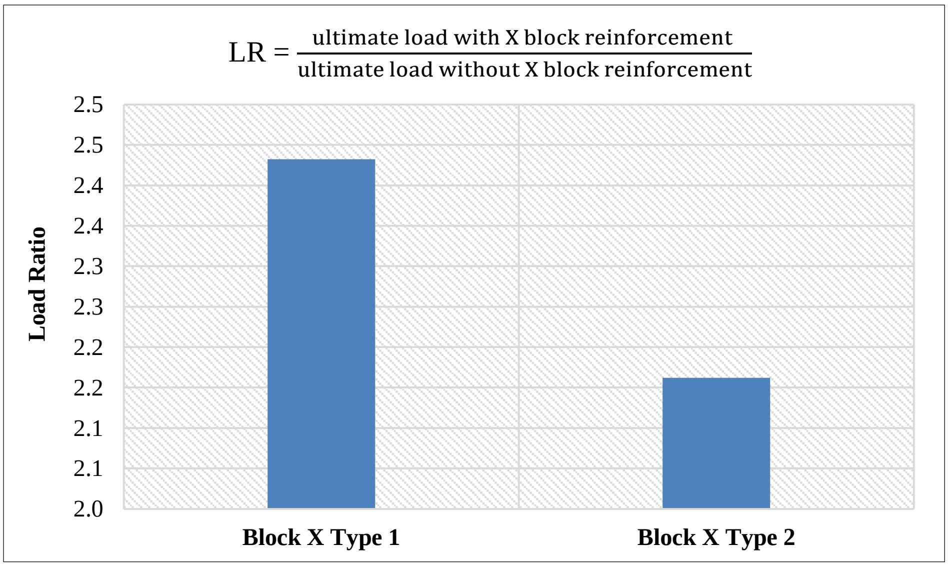

Figure 10. The load ratio of both X-block

5. Conclusion

Based on the analysis of the slope testing results, it is possible to infer that the results of the creation of the type X-block design, which was used as a retaining wall material, were capable of efficiently resisting landslides on the slopes under consideration. Based on the results, the horizontal deformation value is quite minimal when compared to the height of the slope. This also shows that X-Block type 1 performs better as slope reinforcement than X-Block type 2 since it has a lower horizontal and vertical deformation ratio. The rise in slope stability based on the ratio of the X-block reinforcement's ultimate load ratio and the load just before failure is 2.4 for the X-block type 1 reinforcement and 2.2 for the X-block type 2 reinforcement. This ratio indicates that the X-type blocks 1 and 2 can withstand a load twice as great as the failure load. This number also demonstrates that X-Block type 1 is more effective than X-Block type 2. As a result, the safety factor increased by 2.73 after being strengthened with type X beams for both X-block type 1 and X-block type 2. In general, X-block utilization in slope stability should be widely considered due to its capability of increasing the slope load capacity, especially in areas with very soft soil and high slopes.

6. Declarations

6.1. Author Contributions

Conceptualization, E.K. and T.H.; methodology, E.K.; software, E.K.; validation, T.H., A.B.M. and R.I.; formal analysis, E.K.; investigation, E.K.; resources, E.K.; data curation, E.K.; writing—original draft preparation, E.K.; writing—review and editing, E.K.; visualization, E.K.; supervision, T.H.; project administration, E.K. All authors have read and agreed to the published version of the manuscript.

6.2. Data Availability Statement

The data presented in this study are available in article.

6.3. Funding and Acknowledgment

The author wishes to convey a heartfelt gratitude and appreciation to BPPDN (Domestic Postgraduate Education Scholarship). The authors would also like to thank the supervising lecturers who gave direction and advice so that this study could be finished appropriately, as well as all colleagues at Hasanuddin University Indonesia's Geotechnical Laboratory who were engaged in this research from start to finish.

6.4. Conflicts of Interest

The authors declare no conflict of interest.

7. References

[1] Rossi, M., Guzzetti, F., Salvati, P., Donnini, M., Napolitano, E., & Bianchi, C. (2019). A predictive model of societal landslide risk in Italy. Earth-Science Reviews, 196. doi:10.1016/j.earscirev.2019.04.021.

[2] Akgun, A. (2012). A comparison of landslide susceptibility maps produced by logistic regression, multi-criteria decision, and likelihood ratio methods: A case study at İzmir, Turkey. Landslides, 9(1), 93–106. doi:10.1007/s10346-011-0283-7.

[3] Salvati, P., Petrucci, O., Rossi, M., Bianchi, C., Pasqua, A. A., & Guzzetti, F. (2018). Gender, age and circumstances analysis of flood and landslide fatalities in Italy. Science of the Total Environment, 610–611, 867–879. doi:10.1016/j.scitotenv.2017.08.064.

[4] Harianto, T., Yunus, M., & Walenna, M. A. (2021). Bearing Capacity of Raft-Pile Foundation Using Timber Pile on Soft Soil. International Journal of GEOMATE, 21(86), 108–114. doi:10.21660/2021.86.j2294.

[5] Zhang, M., & McSaveney, M. J. (2018). Is air pollution causing landslides in China? Earth and Planetary Science Letters, 481, 284–289. doi:10.1016/j.epsl.2017.10.045.

[6] Harianto, T., Hamzah, S., Nur, S. H., Abdurrahman, M. A., Latief, R. U., Fadliah, I., & Walenna, A. (2013, September). Biogrouting stabilization on marine sandy clay soil. Proceedings of the 7th International Conference on Asian and Pacific Coasts, Indonesia.

[7] Fattet, M., Fu, Y., Ghestem, M., Ma, W., Foulonneau, M., Nespoulous, J., Le Bissonnais, Y., & Stokes, A. (2011). Effects of vegetation type on soil resistance to erosion: Relationship between aggregate stability and shear strength. Catena, 87(1), 60–69. doi:10.1016/j.catena.2011.05.006.

[8] Harianto, T., Samang, L., Suheriyatna, Y. S., & Sandyutama, Y. (2016). Field Investigation of the Performance of Soft Soil Reinforcement with Inclined Pile. In 5th International Conference on Geotechnical and Geophysical Site Characterisation, Queensland, Australia.

[9] Erdawaty, Harianto, T., Muhiddin, A. B., & Arsyad, A. (2020). Experimental study on bearing capacity of alkaline activated granular asphalt concrete columns on soft soils. Civil Engineering Journal (Iran), 6(12), 2363–2374. doi:10.28991/cej-2020-03091623.

[10] Liu, S., Fan, K., & Xu, S. (2019). Field study of a retaining wall constructed with clay-filled soilbags. Geotextiles and Geomembranes, 47(1), 87–94. doi:10.1016/j.geotexmem.2018.11.001.

[11] Muhiddin, A. B., & Tangkeallo, M. M. (2020). Correlation of unconfined compressive strength and California bearing ratio in laterite soil stabilization using varied zeolite content activated by waterglass. Materials Science Forum, 998 MSF, 323–328. doi:10.4028/www.scientific.net/MSF.998.323.

[12] Wang, X., & Niu, R. (2009). Spatial forecast of landslides in Three Gorges based on spatial data mining. Sensors, 9(3), 2035–2061. doi:10.3390/s90302035.

[13] Raghuvanshi, T. K., Ibrahim, J., & Ayalew, D. (2014). Slope stability susceptibility evaluation parameter (SSEP) rating scheme - An approach for landslide hazard zonation. Journal of African Earth Sciences, 99(PA2), 595–612. doi:10.1016/j.jafrearsci.2014.05.004.

[14] Ayalew, L., Yamagishi, H., & Ugawa, N. (2004). Landslide susceptibility mapping using GIS-based weighted linear combination, the case in Tsugawa area of Agano River, Niigata Prefecture, Japan. Landslides, 1(1), 73–81. doi:10.1007/s10346-003-0006-9.

[15] Gorsevski, P. V., Jankowski, P., & Gessler, P. E. (2006). An heuristic approach for mapping landslide hazard by integrating fuzzy logic with analytic hierarchy process. Control and Cybernetics, 35(1), 121-146.

[16] Casagli, N., Catani, F., Puglisi, C., Delmonaco, G., Ermini, L., & Margottini, C. (2004). An inventory-based approach to landslide susceptibility assessment and its application to the Virginio River Basin, Italy. Environmental and Engineering Geoscience, 10(3), 203–216. doi:10.2113/10.3.203.

[17] di Lernia, A., Cotecchia, F., Elia, G., Tagarelli, V., Santaloia, F., & Palladino, G. (2022). Assessing the influence of the hydraulic boundary conditions on clay slope stability: The Fontana Monte case study. Engineering Geology, 297. doi:10.1016/j.enggeo.2021.106509.

[18] Azarafza, M., Akgün, H., Ghazifard, A., Asghari-Kaljahi, E., Rahnamarad, J., & Derakhshani, R. (2021). Discontinuous rock slope stability analysis by limit equilibrium approaches–a review. International Journal of Digital Earth, 14(12), 1918–1941. doi:10.1080/17538947.2021.1988163.

[19] Liu, Z., Wang, X., Yin, Y., Li, J., & Shao, G. (2022). Stability analysis of an unsaturated clay slope based on the coupled effect of temperature and saturation. Quarterly Journal of Engineering Geology and Hydrogeology, 55(2), 1-14. doi:10.1144/qjegh2021-009.

[20] Dawson, E.M., & Roth, W.H. (2020). Slope stability analysis with FLAC. FLAC and Numerical Modeling in Geomechanics. CRC Press, Florida, United States. doi:10.1201/9781003078531-2.

[21] Zhou, J., Li, E., Yang, S., Wang, M., Shi, X., Yao, S., & Mitri, H. S. (2019). Slope stability prediction for circular mode failure using gradient boosting machine approach based on an updated database of case histories. Safety Science, 118, 505–518. doi:10.1016/j.ssci.2019.05.046.

[22] Qi, C., & Tang, X. (2018). Slope stability prediction using integrated metaheuristic and machine learning approaches: A comparative study. Computers and Industrial Engineering, 118, 112–122. doi:10.1016/j.cie.2018.02.028.

[23] Salmasi, F., Chamani, M. R., & Farsadi Zadeh, D. (2012). Experimental study of energy dissipation over stepped gabion spillways with low heights. Iranian Journal of Science and Technology - Transactions of Civil Engineering, 36(C2), 253–264. doi: 10.22099/IJSTC.2012.640.

[24] Najafzadeh, M., Rezaie-Balf, M., & Tafarojnoruz, A. (2018). Prediction of riprap stone size under overtopping flow using data-driven models. International Journal of River Basin Management, 16(4), 505–512. doi:10.1080/15715124.2018.1437738.

[25] Mohamed, M. H., Ahmed, M., & Mallick, J. (2021). An experimental study of nailed soil slope models: Effects of building foundation and soil characteristics. Applied Sciences (Switzerland), 11(16), 4842. doi:10.3390/app11167735.

[26] Irmawaty, R., Djamaluddin, R., & Akkas, A. M. (2014). Bending Capacity of Styrofoam Filled Concrete (SFC) Using Truss System Reinforcement. In Conference for Civil Engineering Research Networks (CONCERN), Bandung, Indonesia.